Ono et al., http://www.jcb.org/cgi/content/full/jcb.201208008/DC1

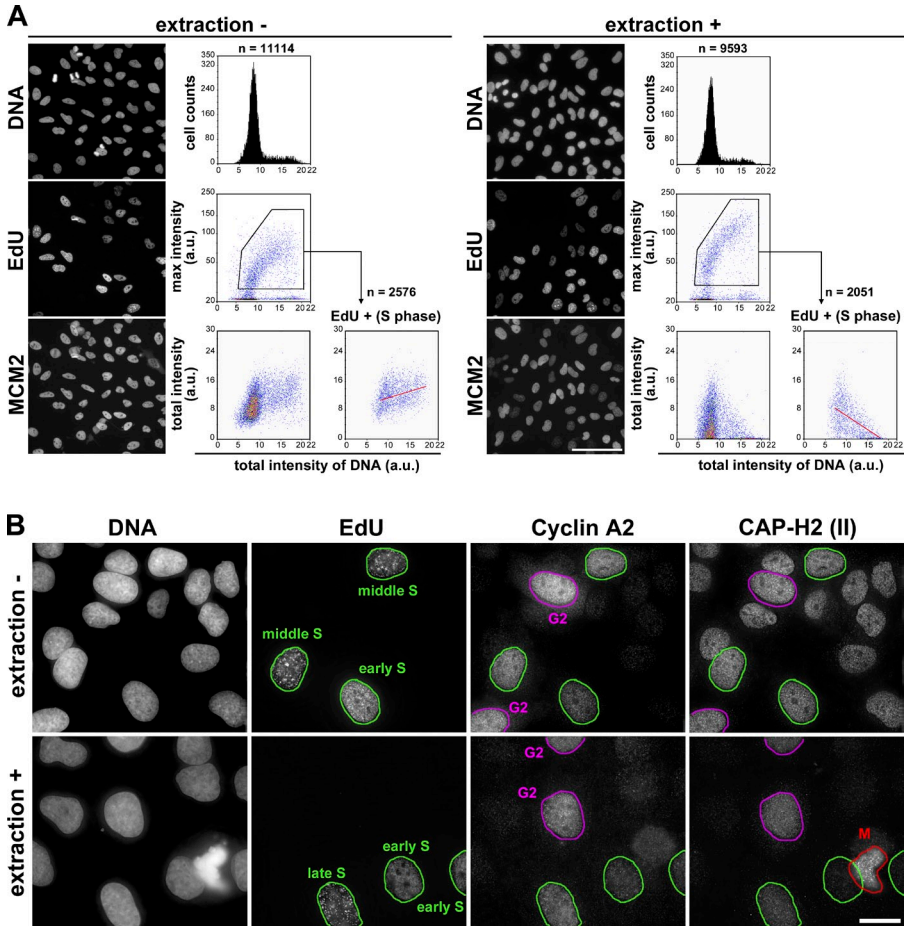

Figure S1. **Chromatin-binding properties of MCM2 and condensin II during the cell cycle.** (A) Quantitative imaging analyses of MCM2 using CELAVIEW RS100 (Olympus). Asynchronous HeLa cells were labeled with EdU for 0.5 h and fixed directly (extraction −) or fixed after extraction (extraction +). The cells were treated with the Click-iT EdU imaging kits (Invitrogen), and then immunolabeled with anti-human MCM2 (BM28; BD). DNA was counterstained with DAPI. Bar, 100 µm. The first row shows DAPI-stained images and profiles of total intensity of DNA per nucleus (x axis) and cells counted (y axis). The second row shows the EdU-labeled images and scattergrams of DNA intensity and max intensity of EdU. The data included in the pentagonal area were judged to be S phase cells. The third row shows MCM2-labeled images and the distribution of the total nuclear intensity of MCM2 in the whole cell cycle population (left) or in the S phase population (right, EdU +). Consistent with a previous study (Dimitrova et al., 1999), although the whole fraction of MCM2 gradually increased during S phase progression (extraction −), the chromatin-bound (extraction-resistant) fraction of MCM2 decreased (extraction +). In the scattergrams of EdU-positive cells, regression lines were drawn in red. (B) Additional evidence that condensin II starts to associate with chromatin during S phase. Asynchronously grown HeLa cells were pulse labeled with EdU for 0.5 h, fixed directly (extraction −) or fixed after extraction (extraction +), and treated with the Click-iT EdU imaging kits (Invitrogen). The cells were then immunolabeled with mouse monoclonal anti-human cyclin A2 and anti-human CAP-H2. DNA was counterstained with DAPI. Bar, 10 µm. On the basis of the labeling patterns of EdU and cyclin A2, cell cycle stages were judged as G1 (not marked), S phase (green), G2 (magenta), and mitosis (red; Pines and Hunter, 1991; Furuno et al., 1999). Without prior extraction (extraction −), the signal level of CAP-H2 was relatively constant from G1 through G2. In the cell population subjected to extraction before fixation (extraction +), however, the signal level of CAP-H2 increased during S phase and got higher in G2.

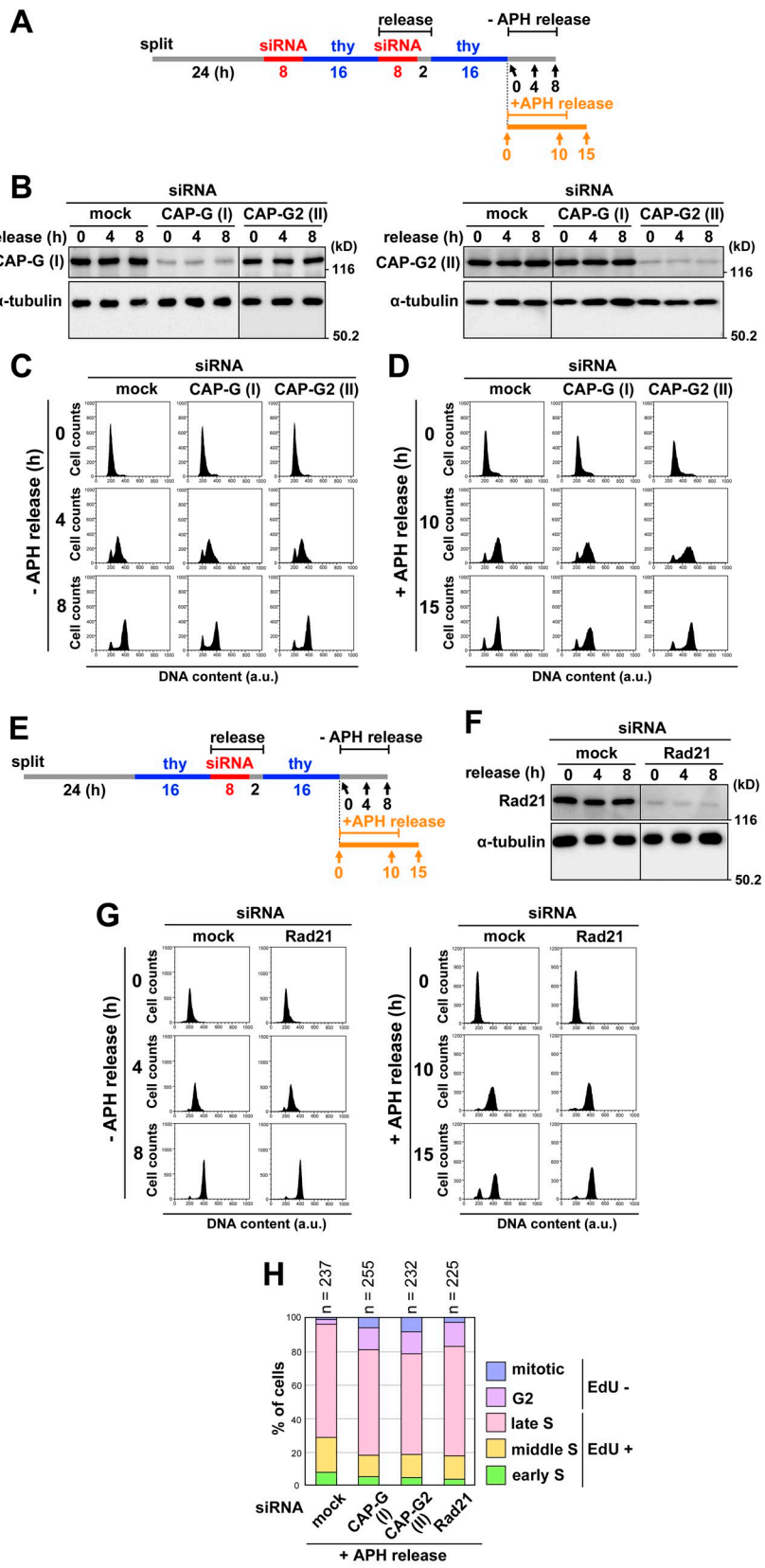

Figure S2. **S phase progression is barely affected by depletion of condensins or cohesin in the absence or presence of mild replicative stress.** (A) Experimental protocol for siRNA-mediated depletion of condensin subunits from synchronous HeLa cell cultures, followed by release into a medium containing no aphidicolin (−APH) or 0.1 µg/ml aphidicolin (+APH). The cells were harvested and processed for FACS and immunoblotting analyses at the time points indicated by the arrows. (B) Whole cell lysates were prepared from the culture released in the absence of aphidicolin and analyzed by immunoblotting with antibodies against CAP-G, CAP-G2, and α-tubulin. (C) Synchronized cells mock depleted or depleted of CAP-G or CAP-G2 were released in the absence of aphidicolin and subjected to FACS analysis. (D) Synchronized cells mock depleted or depleted of CAP-G or CAP-G2 were released in the presence of aphidicolin and subjected to FACS analysis. (E) Experimental protocol for siRNA-mediated depletion of cohesin from a synchronous HeLa cell culture, followed by release into a medium in the absence (−APH) or presence (+APH) of 0.1 µg/ml aphidicolin. The cells were harvested and processed for immunoblotting and FACS analyses at the time points indicated by the arrows. (F) Whole cell lysates were prepared from the culture released in the absence of aphidicolin and analyzed by immunoblotting with antibodies against human Rad21 (Gandhi et al., 2006) and α-tubulin. (G) Synchronized cells depleted of Rad21 were released in the absence (left; −APH release) or presence (right; +APH release) of aphidicolin and subjected to FACS analysis. (H) HeLa cells were released from the second thymidine block in the presence of 0.1 µg/ml aphidicolin for 12.5 h (+APH) and pulse labeled with EdU for 0.5 h before harvest, as described in Fig. 5 E. Plotted here are cell cycle stages of the aphidicolin-treated cells that were judged on the basis of the EdU-labeling pattern and cell morphology. The data shown are from a single representative experiment out of two repeats.

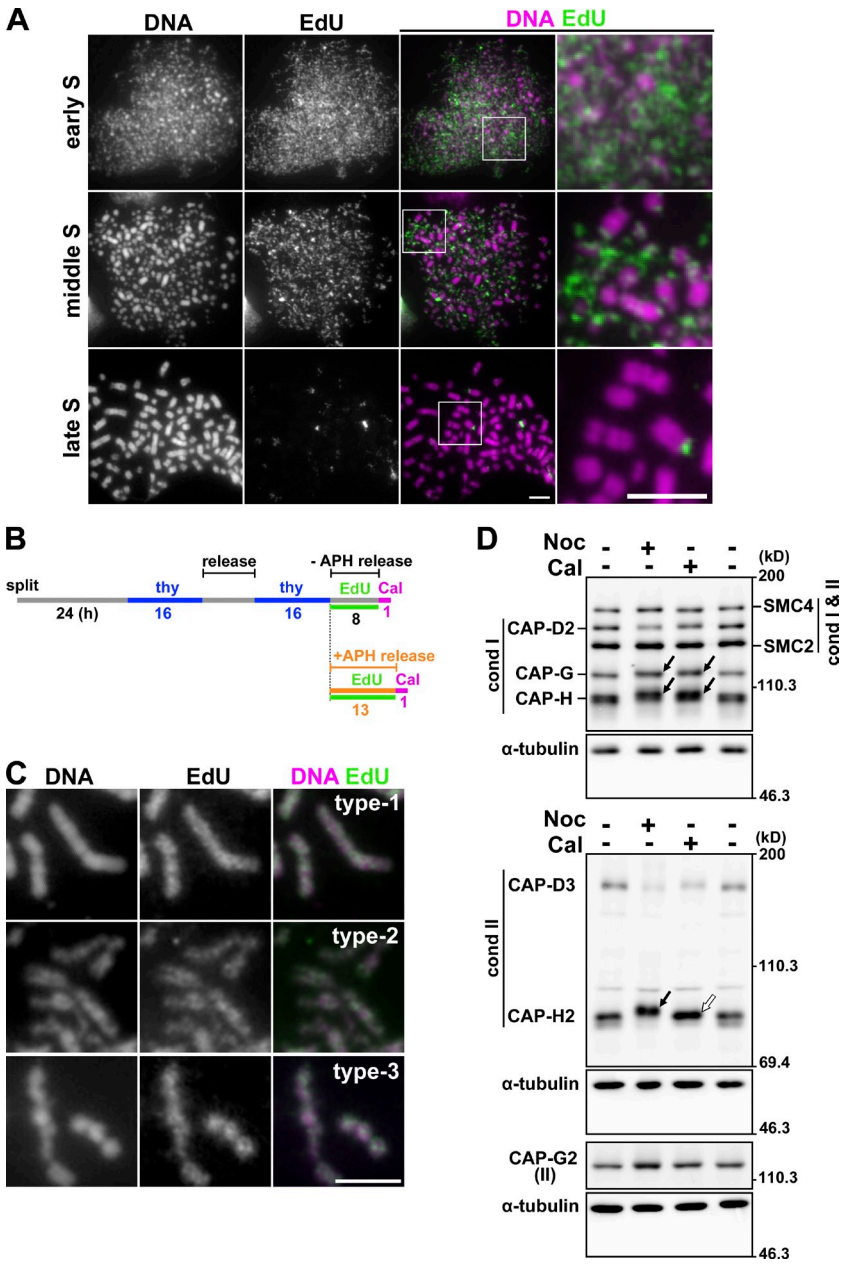

Figure S3. **Calyculin A–induced S-PCC products in HeLa cells.** (A) Asynchronously grown, mock-depleted HeLa cells (described in Fig. 3 A) were treated with a hypotonic solution, fixed with Carnoy's solution, and then spread onto glass slides. The slides were treated with the Click-iT EdU imaging kits and stained with DAPI. Shown here are representative images of early S-, middle S-, and late S-PCC cells. Closeups of the images indicated by the white boxes are shown in the right. Bars, 5 µm. (B) Experimental protocol for detection of replicated regions by continuous labeling with EdU. After the second block of thymidine, HeLa cells were released into a medium containing no aphidicolin (−APH) or 0.1 µg/ml aphidicolin (+APH) in the presence of 0.1 µM EdU. The cells were treated with calyculin A for 1 h at the indicated time points before fixation and treated as described in Fig. 5 B. (C) Shown here are representative images of the three different types of late S-PCC products (see Fig. 5 B and the text for details). Despite the morphological differences, EdU signals were detected uniformly in the entire regions of all three types of chromosomes. Together with the data shown in Fig. S2, we can exclude the possibility that the severe resolution defects observed here are caused by a failure of bulk chromosomal replication. Bar, 5 µm. (D) Whole cell lysates were prepared from asynchronously grown cultures in the presence or absence of 50 ng/ml nocodazole (for 16 h) or 50 nM calyculin A (for 1 h) and analyzed by immunoblotting with antibodies against the core subunits of condensins (SMC2 and SMC4; Kimura et al., 2001), condensin I–specific subunits (CAP-D2, -G, and -H; Kimura et al., 2001), and condensin II–specific subunits (CAP-D3, -G2, and -H2; Ono et al., 2003). α-Tubulin was used as a loading control. Upon treatment with calyculin A, CAP-G and -H (condensin I) were shifted in a manner indistinguishable from that observed in the presence of nocodazole (top, black arrows). In contrast, the mobility shift of CAP-H2 (condensin II) induced by treatment with calyculin A (third panel, white arrow) was far less prominent than that induced by nocodazole treatment (third panel, black arrow).

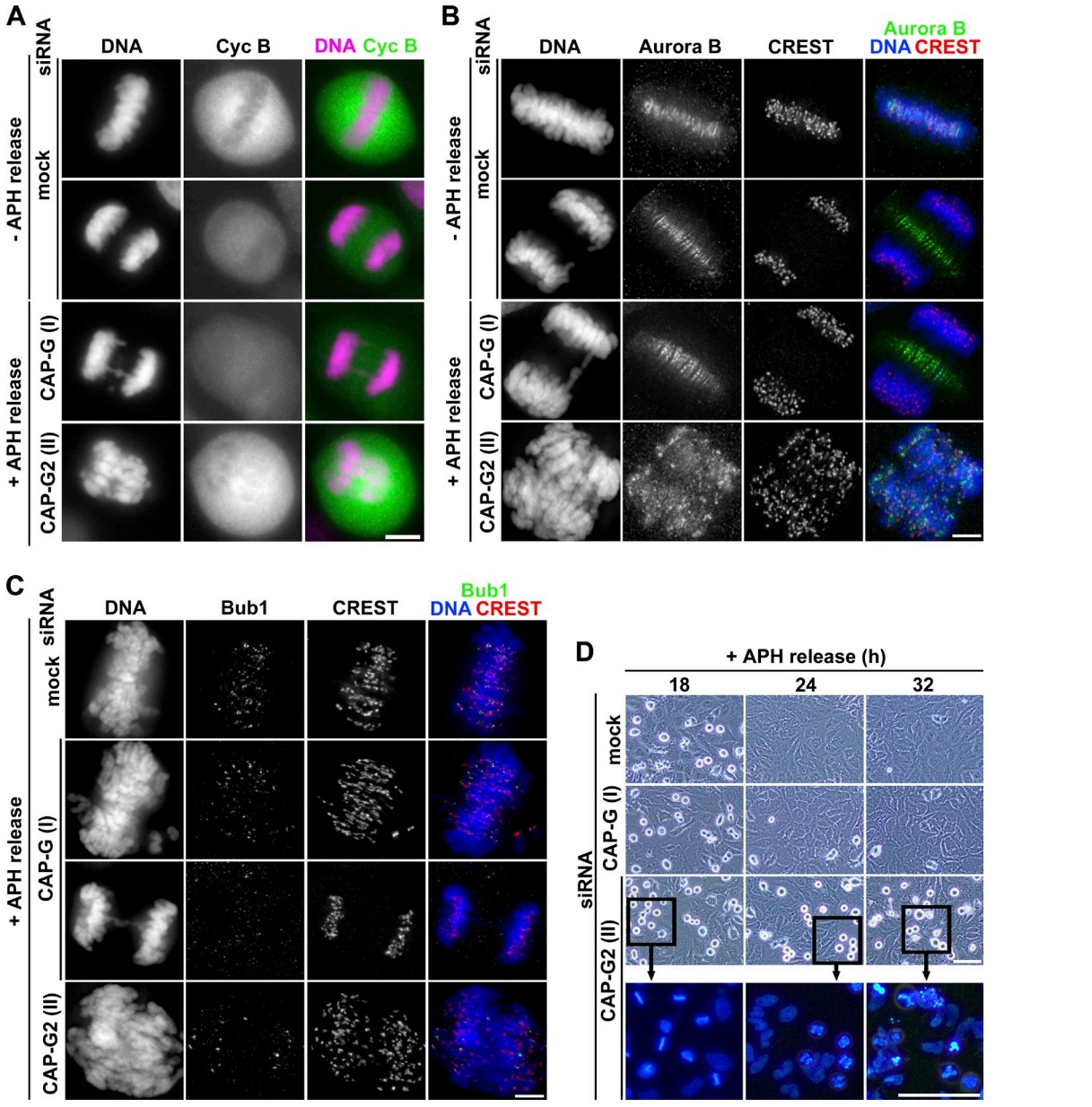

Figure S4. **Application of mild replicative stress in condensin II–depleted cells causes a pseudometaphase arrest and cell death.** Mitotic HeLa cells from siRNA-treated synchronized cultures were prepared as described in Fig. 6 D. After the second thymidine block, the cultures were released into a medium containing no aphidicolin (−APH) or 0.1 µg/ml aphidicolin (+APH) and allowed to enter into mitosis before fixation. (A) The cells fixed on coverslips were immunolabeled with anti–cyclin B1 (Santa Cruz Biotechnology, Inc.). Shown here are representative images from the selective conditions as indicated in the left: normal metaphase and anaphase cells (first and second rows), an anaphase cell with chromosome bridges (third row), and a cell with cotton candy chromosomes (fourth row). Bar, 10 µm. (B) The same set of cells was immunolabeled with anti–Aurora B (anti–hAIM-1; BD) and CREST serum. Shown here are representative images as described in A. Bar, 5 µm. (C) The same set of cells was immunolabeled with anti-Bub1 (MBL) and CREST serum. Shown here are representative images from the selected conditions as indicated in the left: a metaphase cell with aligned chromosomes (first row), a metaphase cell with poorly aligned chromosomes (second row), an anaphase cell with chromosome bridges (third row), and a cell with cotton candy chromosomes (fourth row). Bar, 5 µm. (D) The same set of cultures was incubated for a long period and observed by phase-contrast microscopy at the time points indicated. Shown in the bottom are Hoechst 33342–stained closeups of the regions indicated by the black boxes in the third row. Bars, 100 µm.

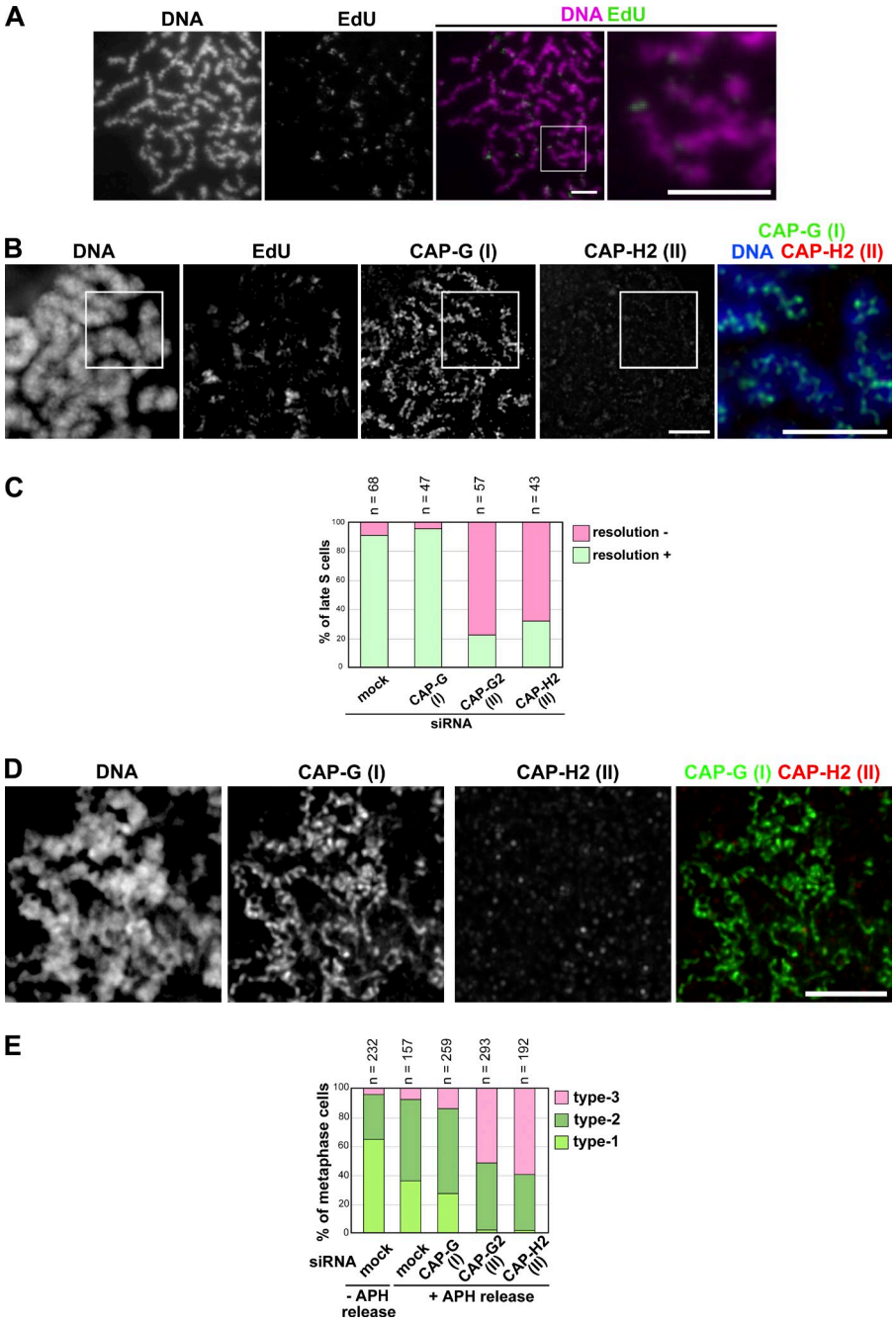

Figure S5. **Additional evidence that condensin II contributes to sister chromatid resolution during S phase.** (A) The same set of experiments described in Fig. 3 B was performed with HeLa cells depleted of CAP-H2, another subunit of condensin II. Shown here is a representative image of late S-PCC cells. Closeups of the images indicated by the white boxes are shown in the right. Depletion of CAP-H2 caused a defective phenotype indistinguishable from that observed in CAP-G2–depleted cells (Fig. 3 B, CAP-G2 siRNA): chromosomes were grossly wavy and sister chromatids were hardly recognizable. Bars, 5 µm. (B) The same set of experiments described in Fig. 3 C was performed with HeLa cells depleted of CAP-H2. Shown here is a representative image of late S-PCC cells. Closeups of the images indicated by the white boxes are shown in the right. Again, the cells depleted of CAP-H2 displayed similar defects observed in the cells depleted of CAP-G2 (Fig. 3 C, CAP-G2 siRNA): CAP-G–positive axes were distorted and poorly resolved, whereas CAP-H2 signals were barely detectable. Bars, 5 µm. (C) Plotted here is the frequency of resolution defects in late S-PCC products in the cells depleted of CAP-H2. This quantitative evaluation was completed once. For comparison with the cells mock depleted or depleted of other subunits of condensins the plot shown in Fig. 3 D is duplicated here. (D) The same set of experiments described in Fig. 6 B was performed with HeLa cells depleted of CAP-H2. Shown here is a representative image of metaphase chromosome spreads prepared from synchronized cells depleted of CAP-H2 and released in the presence of 0.1 µg/ml aphidicolin. Depletion of CAP-H2 caused a similar defect to that observed in CAP-G2–depleted cells (Fig. 6 B, +APH release, CAP-G2 siRNA): continuous axial structures were no longer visible and sister chromatids were barely recognizable. Bar, 5 µm. (E) Plotted here is the frequency of metaphase defects observed in the cells depleted of CAP-H2 released in the presence of aphidicolin. For the classification of the three types, see Fig. 6 C and the main text. The data shown are from a single representative experiment out of two repeats. For comparison with the cells mock depleted or depleted of other subunits of condensins, the plot shown in Fig. 6 C is duplicated here.

Table S1. **Statistical data of the distance between sister FISH signals (probe 145C4)**

BAC	145C4		
siRNA	**Mock**	**CAP-G**	**CAP-G2**
Number of cells	142	139	136
Minimum*	0.10	0.10	0.10
25%	0.46	0.45	0.14
Median	0.72	0.70	0.41
75%	1.07	1.08	0.71
Maximum	2.83	2.77	3.57
Mean	0.83	0.77	0.53
SD	0.59	0.50	0.47
Standard error	0.05	0.04	0.04

FISH images were acquired with a DeltaVision restoration microscope system (Applied Precision), deconvoluted, and projected (see Materials and methods). The distance between sister FISH signals in the projected images was measured using the softWoRx software (Applied Precision). For reasons of convenience, all values judged to be <0.2 μm, the limit of optical resolution, were treated as 0.1 μm, as indicated by the asterisk. Note that this treatment does not affect the median value in each data set.

Table S2. **Statistical data of the distance between sister FISH signals (probe 10A17)**

BAC	10A17			
siRNA	**Mock**	**CAP-G**	**CAP-G2**	**Rad21**
Number of cells	142	139	140	135
Minimum*	0.10	0.10	0.10	0.10
25%	0.10	0.10	0.10	0.50
Median	0.42	0.39	0.32	0.70
75%	0.60	0.55	0.52	1.02
Maximum	1.22	0.96	1.31	2.33
Mean	0.42	0.38	0.36	0.78
SD	0.25	0.23	0.26	0.45
Standard error	0.02	0.02	0.02	0.04

The data were acquired as described in the legend of Table S1. For reasons of convenience, all values judged to be <0.2 μm, the limit of optical resolution, were treated as 0.1 μm, as indicated by the asterisk. Note that this treatment does not affect the median value in each data set.

Table S3. **Statistical data of the distance between sister FISH signals (probe 285H13)**

BAC	285H13							
	−APH				+APH (0.1 μg/ml)			
siRNA	**Mock**	**CAP-G**	**CAP-G2**	**Rad21**	**Mock**	**CAP-G**	**CAP-G2**	**Rad21**
Number of cells	141	118	117	140	134	138	139	121
Minimum*	0.10	0.10	0.10	0.10	0.10	0.10	0.10	0.10
25%	0.43	0.26	0.10	0.53	0.28	0.10	0.10	0.35
Median	0.66	0.60	0.41	0.81	0.47	0.46	0.32	0.64
75%	0.92	0.97	0.56	1.39	0.71	0.69	0.60	0.91
Maximum	2.08	2.69	1.42	4.34	2.07	2.79	1.88	2.30
Mean	0.68	0.67	0.41	1.00	0.55	0.53	0.39	0.68
SD	0.39	0.52	0.28	0.69	0.42	0.48	0.34	0.46
Standard error	0.03	0.05	0.03	0.06	0.04	0.04	0.03	0.04

The data were acquired as described in the legend of Table S1. For reasons of convenience, all values judged to be <0.2 μm, the limit of optical resolution, were treated as 0.1 μm, as indicated by the asterisk. Note that this treatment does not affect the median value in each data set.

References

Dimitrova, D.S., I.T. Todorov, T. Melendy, and D.M. Gilbert. 1999. Mcm2, but not RPA, is a component of the mammalian early G1-phase prereplication complex. *J. Cell Biol.* 146:709–722. http://dx.doi.org/10.1083/jcb.146.4.709

Furuno, N., N. den Elzen, and J. Pines. 1999. Human cyclin A is required for mitosis until mid prophase. *J. Cell Biol.* 147:295–306. http://dx.doi.org/10.1083/jcb.147.2.295

Gandhi, R., P.J. Gillespie, and T. Hirano. 2006. Human Wapl is a cohesin-binding protein that promotes sister-chromatid resolution in mitotic prophase. *Curr. Biol.* 16:2406–2417. http://dx.doi.org/10.1016/j.cub.2006.10.061

Kimura, K., O. Cuvier, and T. Hirano. 2001. Chromosome condensation by a human condensin complex in *Xenopus* egg extracts. *J. Biol. Chem.* 276:5417–5420. http://dx.doi.org/10.1074/jbc.C000873200

Ono, T., A. Losada, M. Hirano, M.P. Myers, A.F. Neuwald, and T. Hirano. 2003. Differential contributions of condensin I and condensin II to mitotic chromosome architecture in vertebrate cells. *Cell*. 115:109–121. http://dx.doi.org/10.1016/S0092-8674(03)00724-4

Pines, J., and T. Hunter. 1991. Human cyclins A and B1 are differentially located in the cell and undergo cell cycle–dependent nuclear transport. *J. Cell Biol.* 115:1–17. http://dx.doi.org/10.1083/jcb.115.1.1